Preparation, Organophilicity, and Self-Assembly of Poly(oxypropylene)amine−Clay Hybrids

Chih-Cheng Chou,† Fuh-Sheng Shieu,‡ and Jiang-Jen Lin*,†

Department of Chemical Engineering and Department of Materials Engineering, National Chung-Hsing University, Taichung 402, Taiwan

Received October 24, 2002
Revised Manuscript Received February 26, 2003

Materials in the nanoscale (1−100 nm) have received a great deal of attention because of their versatile applications in nanocomposites[1−7] and electronic materials.[8,9] The miniaturization of a material from micrometer to nanometer scale not only dramatically changes in surface-to-weight ratio but also brings out unusual physical and optoelectronic behaviors.[9] Owing to their natural abundance, layered aluminosilicate clays, such as montmorillonite (MMT), are structurally well-defined and commonly used for different applications.[10−12] These clays are sheet unit aggregated particles with dimensions of approximately 100 × 100 × 1 nm for each sheet.[11] Since the disclosure of the nylon-6/clay nanocomposite by the Toyota research group,[10,11,13] a great deal of effort has focused on dispersing inorganic clays into different polymer-layered silicate (PLS) nanocomposites, including polystyrene,[14−16] polypropylene,[17] polyimide,[18] epoxy resin,[19,20] novolac,[5] etc. In general, the preparation involves the intercalation of layered silicates into organoclays by ionic exchange with low molecular weight surfactants, generally up to 30 Å basal spacing.[1−6] In the process of preparing PLS nanocomposites, a general problem arises due to the incompatibility between the ionic MMT and the hydrophobic polymers. Therefore, an intercalating surfactant molecule may be specially designed by incorporating reactive C=C functionalities[21,22] or using polystyrene-based surfactants.[23] Previously, we reported a wide spacing enlargement achieved by using poly(oxypropylene)-amines as the intercalating agents.[24] In this report, we correlate the observed basal spacing to the variants of molecular weight, intercalating site multiplicity, and weight fraction of the intercalating amines including the trifunctional and difunctional amines.

In using poly(oxyethylene) (POE)- and poly(oxypropylene) (POP)-backboned amines, the intercalation of Na^+−MMT was performed. In this study, the POE-amines are the α,ω-diamine of poly(oxypropylene)-*b*-poly(oxyethylene)-*b*-poly(oxypropylene) of 2000 M_w (POE-D2000) and 6000 M_w (POE-D6000). The POP-amines include the poly(oxypropylene)-backboned diamine of 230, 400, 2000, and 4000 M_w (POP-D230, POP-D400, POP-D2000, and POP-D4000, respectively) and the analogous triamines of POP-T400, POP-T3000, and POP-T5000.

The intercalation proceeded via an ionic exchange reaction between the quaternary ammonium salts ($-NH_3^+Cl-$) and sodium ions ($\equiv Si-O^-Na^+$) of MMT.

† Department of Chemical Engineering.
‡ Department of Materials Engineering.
* Corresponding author: Fax +886-4-2287-1787; e-mail JJLin@dragon.nchu.edu.tw.

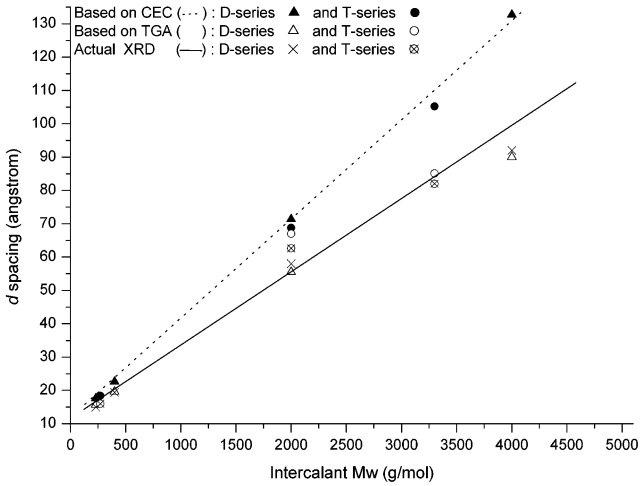

Figure 1. Comparison of actual XRD *d* spacing and from the *d* spacing eq 2 based on CEC or TGA.

When using 1 equiv of POE-amine to the MMT exchange capacity, the *d* spacing increased from the pristine 12.4 to 19.0 Å for 2000 g/mol and 19.8 Å for 6000 g/mol diamine. It appears that these interlayer space distances are independent of molecular weight. On the basis of CEC = 1.15 mequiv/g, the calculated total conversion of the exchangeable ions should amount to a ratio of 2.30 (w/w, organics/silicates) for POE-D2000 and 6.90 (w/w) for POE-D6000. However, the TGA showed only 0.75 and 0.92 (w/w), indicating only 13−33% of ionic exchanging. The low conversion is attributed mainly to the polar nature of the POE backbone. The high affinity of $-(CH_2CH_2O)_x-$ for Na^+ on the silicate plate surface may hinder incoming amines or the completion of the ionic exchange reaction. The resultant POE/MMT hybrids are hydrophilic and dispersible in polar solvents, including water and ethanol.

In contrast to the POE-amines, the hydrophobic POP-amines intercalate MMT differently. Structurally, the POP backbone has a low affinity for silicate surfaces of ionic characteristics. The intercalated MMTs exhibit a *d* spacing of 15.0, 19.4, 58.0, and 92.0 Å, which correlates with their molecular weights of 230, 400, 2000, and 4000 g/mol in a linear relationship (Figure 1, −×−). This implies that each POP-amine intercalates into the MMT in a similar configuration, but differently from the POE-amines. Instead of the POE association with the hydrophilic silicate surface, the POP-amines attach with silicate surfaces only at the tethered quaternary ammonium ion sites. The POP backbones may further self-aggregate through the hydrophobic interactions and consequently stretch out the silicate interlayer gallery.

The use of trifunctional POP-amines provided a variation in molecular configuration in the silicate gallery. In considering the molecular end-to-end distance, the theoretical segment weights between two tethering amines can be estimated to be 270 g/mol for POP-T400 (400/3 × 2 = 270), 2000 g/mol for POP-T3000, and 3300 g/mol for POP-T5000. Their basal spaces were found to be 16.0, 62.6, and 82.0 Å in a linear relationship with their segment weights (Figure 1, −⊗−). Apparently, the length of end-to-end quaternary salts is

10.1021/ma025773h CCC: $25.00
Published on Web 03/13/2003

Table 1. XRD and the Calculated Basal Spacing of POE- and POP-Amine Intercalated MMT

		based on TGA		based on CEC		
intercalation agent[a]	density (g/cm^3)[b]	w/w[d]	*d* spacing (Å)[c]	w/w[d]	*d* spacing (Å)[c]	*d* spacing XRD (Å)
none						12.4
POE-D2000	1.067	0.754	28.8	2.30	67.3	19.0
POE-D6000	1.182	0.923	30.8	6.90	165.3	19.8
POP-D230	0.948	0.204	15.7	0.27	17.6	15.0
POP-D400	0.970	0.351	19.6	0.46	22.6	19.4
POP-D2000	0.996	1.703	55.5	2.30	71.4	58.0
POP-D4000	0.997	3.000	90.0	4.60	132.7	92.0
POP-T400	0.983	0.220	16.0	0.46 (0.31)[e]	22.4 (18.4)	16.0
POP-T3000	1.040	2.230	67.0	3.45 (2.30)	98.2 (68.8)	62.6
POP-T5000	1.062	3.000	85.1	5.75 (3.80)	154.0 (105.2)	82.0

[a] POE = poly(oxyethylene); POP = poly(oxypropylene); D, T = diamine and triamine. [b] Density (g/cm^3) of intercalants, measured in bulk. [c] Calculated *d* spacing by eq 2. [d] w/w: organic fractions from TGA or from CEC (1.15 mequiv/g × M_w). [e] Corrected end-to-end segmental weight in parentheses.

relevant regarding the molecular configuration and consequently the intercalated *d* spacing.

All of the above data were obtained by using 1 equiv of HCl to convert the POP-amines into quaternary salts. In other words, the amine has only one active ionic site attaching to the silicate surface. With the POP-triamines, one to three quaternary ammonium salts in each molecule can associate with the silicate plate and thus alter the configuration in the confinement. To validate this assumption, POP-T5000 was systematically treated with 1−3 equiv of HCl and then subjected to intercalation. The resultant basal spacing differs by 61.0 Å for 3 equiv of HCl, 74.0 Å for 2 equiv of HCl, and 82.0 Å for 1 equiv of HCl. When subjected to 1 equiv of HCl, the POP molecule tethers to the silicate surface at a single site with possibly a bimolecular arrangement, rather than a single molecule alignment with two end attachments to the silicate plates. While multiple ionic sites tether to the silicate plates, the interlayer space tightens to a narrower basal spacing with a constrained POP monolayer. Again, the *d* spacing consistently reflects the end-to-end distance of the molecular configuration in the confined space.

In visualizing the POP-amines in the silicate confinement, the actual incorporated organic portions should occupy the same volume as the silicate gallery. The relationship between interlayer spacing (*D*) and organic weight fraction (*R* or w/w of POP-amine/MMT by weight in Table 1) can be therefore expressed by the following equation

$$D = R\frac{1}{A\rho} + t \qquad (1)$$

where *A* is surface area of montmorillonite, *t* is the plate thickness, and ρ is the density of the POP-amine in the gallery. Substituting the known silicate thickness (t = 10 Å) and surface area (A = 750 m^2/g × $^1/_2$), the equation is transformed as follows:

$$D = R \times \frac{1}{\rho} \times 26.6 + 10 \qquad (2)$$

In the equation, the basal spacing is a function of the intercalant density and its weight fraction. According to this equation, the basal spacing can be derived by adapting the density in bulk and the organic fraction (w/w) which can be obtained either by TGA measurement or by CEC calculation. In regard to the POP-amines (D-series and T-series), the TGA-derived basal spacing correlates well with the actual XRD data (Figure 1, △ and ○). The increasing *d* spacing corresponds with the organic fraction linearly. Hence, the trend represents the consistency of the intercalating mode for each intercalant. In considering the degree of intercalation, the theoretical organics in the intercalated hybrids can be assumed by the known 1.15 mequiv/g MMT cation exchange capacity (CEC) multiplied by the POP molecular weight. By following eq 2, the calculated *d* spacing from CEC represents the theoretical interlayer width corresponding to the intercalant M_w and quantitative ionic exchange. As drawn in Figure 1, the dotted line is above the actual XRD line, particularly for the 4000 g/mol amine intercalation. The discrepancy indicates a lower degree of intercalation with respect to the ionic exchange capacity. The incomplete ionic-exchange reactions can be further estimated by the analyses of Na^+ residue in the washed products. In the pristine Na^+−MMT, the analysis was shown to be 2.31 wt % or 1.00 mequiv/g. After the POP-amine intercalation, the Na^+ content dropped to 0.10 wt % or 0.12

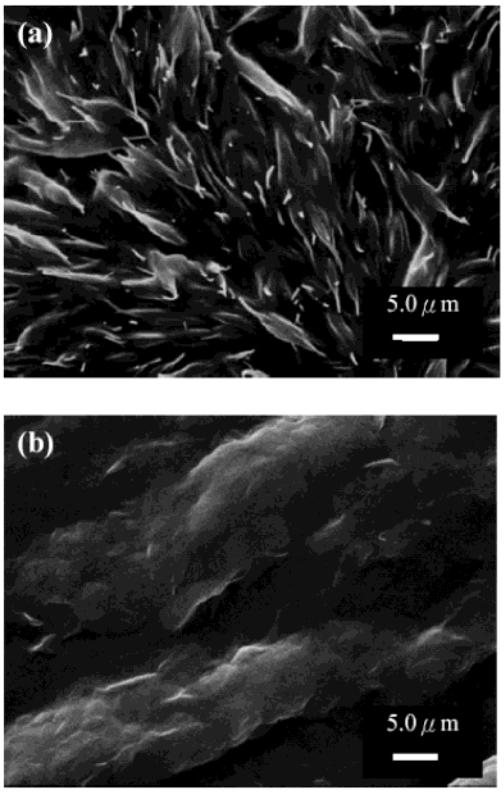

Figure 2. SEM images of POP-D2000 intercalated MMT (a) thin film prepared from self-assembling at toluene/water interface and (b) precipitated aggregates directly from intercalation process.

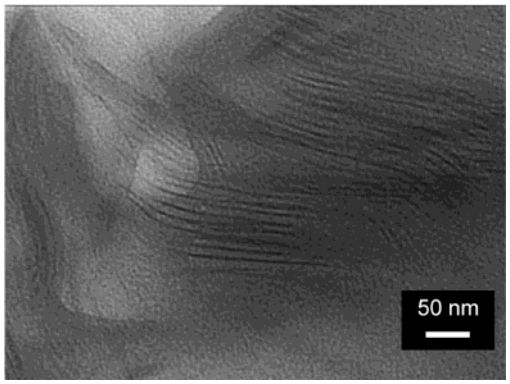

Figure 3. TEM images of POP-D2000 intercalated MMT microstructure of a thin film prepared from self-assembling at the toluene/water interface.

mequiv/g in the case of POP-D2000/MMT. This amounts to 88% of ionic exchange for Na^+−MMT, which is comparable to a 74% of silicate ion coverage on the basis of TGA measurement. In the D-series amines, the organic coverage rate is consistently around 74−76%, except in the case of POP-D4000 (65%). This may be due to the decrease in solubility in water as the POP backbone molecular weight increases, which consequently affects the intercalating process.

The POP/silicate hybrids can be highly hydrophobic, dispersible in toluene, and consisting of an organic fraction up to 75 wt %. The balance of hydrophobic/hydrophilic properties between the POP backbone and the ionic silicate plate rendered the hybrid self-assembling. As an example, the POP-D2000/MMT hybrid, consisting of 63 wt % of organics and 58 Å *d* spacing, enabled to be dispersed in toluene and formed a dimensionally stable film at the toluene/water interface. The film morphology in SEM micrographs was shown to be more structurally oriented than that of the crude powder directly obtained from the precipitation (Figure 2). The TEM micrograph of the film material (Figure 3) clearly shows an orderly layered secondary structure, estimated to be around 55 Å between the layers. The silicate plates stack in 4−10 layers. Moreover, the layers are generally lengthy and have a bending shape. A few layer lengths, estimated over 250 nm, are longer than the expected width of the primary plates (100 nm). Presumably, this fine structure is due to the secondary alignment of the alternating hydrophobic POP organics and hydrophilic silicate plates primary structure.

In conclusion, the intercalation of hydrophobic POP-amines with MMT afforded wide *d* spacing, which is influenced by the orientation of the incorporated organics in the silicate confinement. The *d* spacing is predictable by simply analyzing the incorporated organic fraction. In the silicate confinement, the hydrophobic POP backbones can aggregate in different molecular orientations and further affect the hydrophobic/hydrophilic property.

Acknowledgment. We acknowledge financial support from the National Science Council (NSC) of Taiwan.

References and Notes

(1) Zanetti, M.; Lomakin, S.; Camino, G. *Macromol. Mater. Eng.* **2000**, *279*, 1−9.
(2) Giannelis, E. P. *Appl. Organomet. Chem.* **1998**, *12*, 675−680.
(3) Alexandre, M.; Dubois, P. *Mater. Sci. Eng.* **2000**, *28*, 1−63.
(4) Porter, D.; Metcalfe, E.; Thomas, M. J. K. *Fire Mater.* **2000**, *24*, 45−52.
(5) Wang, H.; Zhao, T.; Zhi, L.; Yan, Y.; Yu, Y. *Macromol. Rapid Commun.* **2002**, *23*, 44−48.
(6) Vaia, R. A.; Ishii, H.; Giannelis, E. P. *Chem. Mater.* **1993**, *5*, 1694−1696.
(7) Strawhecker, K. E.; Manias, E. *Chem. Mater.* **2000**, *12*, 2943−2049.
(8) Kagan, C. R.; Mitzi, D. B.; Dimitrakopoulos, C. D. *Science* **1999**, *286*, 945−947.
(9) Wang, C.; Shim, M.; Sionnest, P. G. *Science* **2001**, *291*, 2390−2392.
(10) Usuki, A.; Kojima, Y.; Kawasumi, M.; Okada, A.; Fukushima, Y.; Kurauchi, T.; Kamigaito, O. *J. Mater. Res.* **1993**, *8*, 1179−1184.
(11) Usuki, A.; Hasegawa, N.; Kadoura, H.; Okamoto, T. *Nano Lett.* **2001**, *1*, 271−272.
(12) Pinnavaia, T. J. *Science* **1983**, *220*, 365−371.
(13) Kojima, Y.; Usuki, A.; Kawasumi, M.; Okada, A.; Kurauchi, T.; Kamigaito, O. *J. Polym. Sci., Polym. Chem.* **1993**, *31*, 1755−1758.
(14) Zhu, J.; Strart, P.; Mauritz, K. A.; Wilkie, C. A. *J. Polym. Sci., Polym. Chem.* **2002**, *40*, 1498−1503.
(15) Fu, X.; Qutubuddin, S. *Polymer* **2001**, *42*, 807−813.
(16) Hasegawa, N.; Okamoto, H.; Kawasumi, M.; Usuki, A. *J. Appl. Polym. Sci.* **1999**, *74*, 3359−3364.
(17) Kawasumi, M.; Hasegawa, N.; Kato, M.; Usuki, A.; Okada, A. *Macromolecules* **1997**, *30*, 6333−6338.
(18) Tyan, H. L.; Liu, Y. C.; Wei, K. H. *Chem. Mater.* **1999**, *11*, 1942−1947.
(19) Lan, T.; Kaviratna, P. D.; Pinnavaia, T. J. *J. Phys. Chem. Solids* **1996**, *57*, 1005−1010.
(20) Triantafillidis, C. S.; LeBaron, P. C. Pinnavaia, T. J. *Chem. Mater.* **2002**, *14*, 4088−4095.
(21) Zeng, C.; Lee, L. J. *Macromolecules* **2001**, *34*, 8978−8985.
(22) Choi, Y. S.; Choi, M. H.; Wang, K. H.; Kim, S. O.; Kim, Y. K.; Chung, I. J. *Macromolecules* **2001**, *14*, 4098−4103.
(23) Beyer, F. L.; Tan, N. C. B.; Dasgupta, A.; Galvin, M. E. *Chem. Mater.* **2002**, *14*, 2983−2988.
(24) Lin, J. J.; Cheng, I. J.; Wang, R.; Lee, R. J. *Macromolecules* **2001**, *34*, 8832−8834.

MA025773H